



Proposal of external modulation scheme for fiber-optic correlation-domain distributed sensing

Kohei Noda^{*}, Giwoon Han, Heeyoung Lee, Yosuke Mizuno, and Kentaro Nakamura

Institute of Innovative Research, Tokyo Institute of Technology, Yokohama 226-8503, Japan

^{*}E-mail: knoda@sonic.pi.titech.ac.jp

Received October 17, 2018; accepted November 23, 2018; published online January 10, 2019

All the previous configurations of optical correlation-domain reflectometry (OCDR) have been based on the direct modulation of laser driving current. However, some lasers are not designed for high-speed large-amplitude modulation, and the modulation amplitude and frequency are mutually dependent. In this work, to mitigate these drawbacks, we propose an external modulation scheme for OCDR. After confirming its basic operation, we show that a non-specially designed laser can be employed. We also clarify that the interdependence of the modulation amplitude and frequency is negligibly small in this scheme, which is not the case for the conventional direct modulation scheme.

© 2019 The Japan Society of Applied Physics

One of the useful techniques for monitoring the soundness of optical components, modules, and fiber networks is optical reflectometry, which has been used to perform multiplexed sensing,^{1,2)} distributed sensing,^{3–5)} and optical coherence tomography.^{6–8)} To detect low-quality connections (or splices) and other reflection points along an optical fiber, optical time-domain reflectometry (OTDR)^{9–13)} and optical frequency-domain reflectometry (OFDR)^{14–18)} have been widely studied. However, OTDR suffers from a relatively low spatial resolution determined by the optical pulse width and a long measurement time, and OFDR generally suffers from phase fluctuations caused by environmental disturbance; in addition, random access to sensing positions is not available in these techniques. One of the methods for mitigating these shortcomings is optical correlation (or coherence)-domain reflectometry (OCDR),^{19–30)} which operates based on the synthesis of optical coherence functions (SOCF).²⁸⁾ In SOCF, optical frequency is modulated in a sinusoidal manner^{21–25)} or in a stepwise manner^{26–28)} including optical frequency comb.^{29,30)} Here, we focus on SOCF-OCDR based on sinusoidal modulation, which has been most widely studied owing to its ease of implementation and cost efficiency.^{21–25)}

To date, all of the SOCF-OCDR configurations have been implemented by directly modulating the driving current of the laser to modulate the optical output-frequency.^{21–25)} Although this direct modulation scheme can be relatively easily implemented, it has following three drawbacks: (i) some lasers are not designed for high-speed large-amplitude modulation of its driving current (and thus, a suitable laser needs to be selected to achieve stable operation), (ii) optical frequency modulation inevitably accompanies optical power modulation (and thus, an unintended apodization effect may deteriorate the performance),^{31,32)} and (iii) the modulation amplitude and frequency are mutually dependent and it is difficult to independently control one of the two (and thus, the actual spatial resolution may largely alter according to the sensing position).

In this work, to mitigate these drawbacks, we propose an external modulation scheme for SOCF-OCDR and confirm its basic operation. Subsequently, focusing on the drawbacks (i) and (iii), first, we show that a laser not designed for special use can be employed in this scheme. We then measure the mutual dependence of the modulation amplitude and the frequency in both the direct and external modulation

schemes, and show that, unlike in the direct modulation scheme (in which the modulation amplitude is sometimes even doubled by the change in the modulation frequency), these parameters are almost independent of each other in the external modulation scheme.

In SOCF-OCDR,^{21–25)} optical frequency is modulated to generate periodical correlation peaks along a fiber under test (FUT), enabling selective detection of the reflection signal from an arbitrary position. A distributed measurement is performed by controlling the modulation frequency f_m to scan one of the correlation peaks along the FUT. The measurement range of the system D is determined by the interval of the correlation peaks and given by²⁸⁾

$$D = \frac{c}{2nf_m}, \quad (1)$$

where c is the light velocity in vacuum, and n is the refractive index of the fiber core. The spatial resolution Δz is given by^{28,33)}

$$\Delta z \cong \frac{0.76c}{\pi n \Delta f}, \quad (2)$$

where Δf is the modulation amplitude. According to Eq. (2), it is clear that, in theory, the spatial resolution is kept constant regardless of the sensing position during distributed measurement (later in this paper, this will be shown not to be necessarily true in practical systems). In conventional SOCF-OCDR, frequency-modulated light was generated by directly modulating the driving current of the laser. However, as this direct modulation scheme poses three aforementioned shortcomings, here we propose an external modulation scheme.

A conceptual setup of the external modulation scheme of OCDR is schematically shown in Fig. 1. The optical parts after dividing the laser output into two beams are basically the same as those of the direct modulation scheme.^{21–25)} In the external modulation scheme, instead of directly modulating the laser driving current, a double-sideband modulator (DSBM) and an optical band-pass filter are employed to modulate the optical frequency. The optical frequency shift corresponds to the frequency of the microwave applied from a voltage-controlled oscillator (VCO) to the DSBM. By controlling the VCO-applied voltage using a function generator, this frequency shift can be swept at high-speed.

To start with, a basic operation of OCDR, i.e., a distributed reflectivity measurement was demonstrated using the external

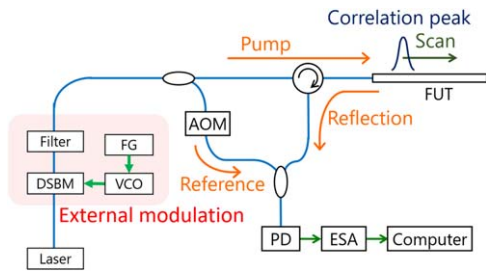


Fig. 1. (Color online) Conceptual schematic of optical correlation-domain reflectometry (OCDR) based on external modulation. AOM: acousto-optic modulator, DSBM: double-sideband modulator, ESA: electrical spectrum analyzer, FG: function generator, PD: photo diode, VCO: voltage-controlled oscillator.

modulation scheme. A distributed-feedback laser diode (NX8563LB, NEC) operating at 1550 nm with a 3 dB line-width of ~ 1 MHz was used. The VCO (HMC733LC4B, Analog Devices) had a wide output-frequency range from 10 to 21 GHz. The optical band-pass filter (BVF-300CL, Alnair) had an edge roll-off of 12 dB GHz^{-1} and was used to select only the upper sideband. In the actual experiment, several optical devices were additionally employed compared with the conceptual setup shown in Fig. 1. An erbium-doped fiber amplifier was inserted in the pump path (output power: $\sim 25 \text{ dBm}$), and a polarization controller (PCTRL) was inserted in the reference path so that the relative polarization state between the reflected light and the reference light was optimized. An acousto-optic modulator was not inserted in the reference path; instead, the foot of the Fresnel reflection spectrum was exploited.²⁴ Using a zero-span function of an electrical spectrum analyzer (ESA) with a sweep rate of 10 Hz, the electrical spectral power at 2.4 MHz was transmitted to a virtual oscilloscope (OSC) in a computer to derive the reflectivity distribution along the FUT (see Ref. 24 for the detail). The resolution and video bandwidths of the ESA were 300 kHz and 1 kHz, respectively. Averaging was performed 128 times on the OSC. The modulation frequency was 3.41–3.60 MHz, and the modulation amplitude was 0.175 GHz, which corresponded to the measurement range of $\sim 30 \text{ m}$ and the spatial resolution of 0.28 m.

The structure of the FUT is depicted in Fig. 2(a). A 4.1, 5.0, 3.0, and 2.1 m long silica single-mode fibers (SMFs) were sequentially connected using two physical contact (PC) connectors and an angled PC (APC) connector. A bending loss was artificially applied in the 2.1 m long SMF to suppress the extremely large Fresnel-reflected signal at the end of the FUT, which was kept open with a PC connector. The reflectivity distribution measured using the external modulation scheme is shown in Fig. 2(b). The horizontal axis indicates the relative position from the proximal PC connector. The vertical axis indicates the relative electrical power, which was normalized so that the maximal and minimal plots became 1 and 0, respectively. Four peaks were clearly observed, the positions of which well agreed with the locations of the connectors. The peak at $\sim 5.0 \text{ m}$ was smaller than the other peaks, which is natural considering that the reflected signal from the APC connector was weaker than those from the PC connectors. Thus, a basic operation of OCDR with the external modulation scheme was confirmed (the detailed characterization of the distributed sensing performance is out of the scope of this paper).

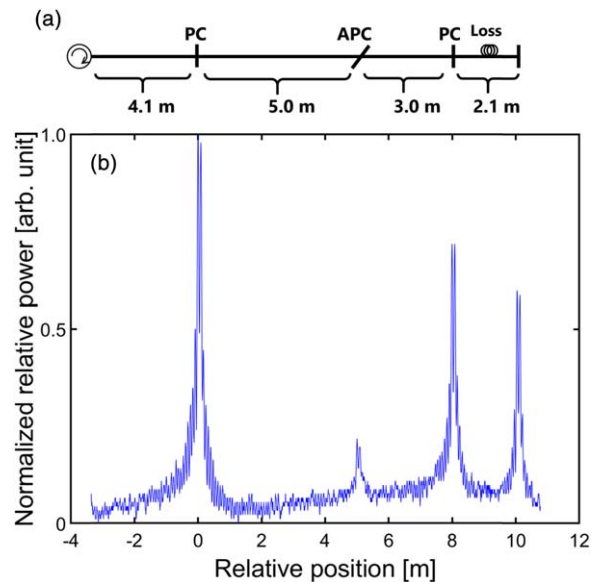


Fig. 2. (Color online) Confirmation of the basic operation of OCDR based on external modulation. (a) Structure of the fiber under test (FUT). APC: angled physical contact, PC: physical contact. (b) Measured distribution of the normalized relative reflection power along the FUT.

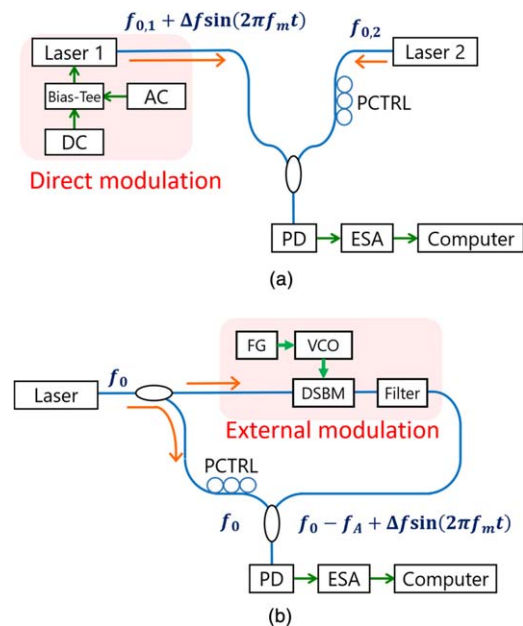


Fig. 3. (Color online) Experimental setups used to characterize (a) the direct modulation scheme and (b) the external modulation scheme. AC: alternating current, DC: direct current, PCTRL: polarization controller.

Subsequently, we focus on the third disadvantage (iii) of the conventional direct modulation scheme, i.e., the nature that the modulation amplitude and frequency are dependent on each other and that the actual spatial resolution varies according to the sensing position. In order to experimentally evaluate this point in both the direct and external modulation schemes, we observed the power spectra and investigated the relation between the modulation frequency and amplitude using setups depicted in Fig. 3(a) (direct modulation scheme) and Fig. 3(b) (external modulation scheme). In the direct modulation scheme, the output from the modulated laser (NX8563LB, NEC) at $\sim 1550 \text{ nm}$ was heterodyned with the output from another tunable laser and the beat spectrum (set

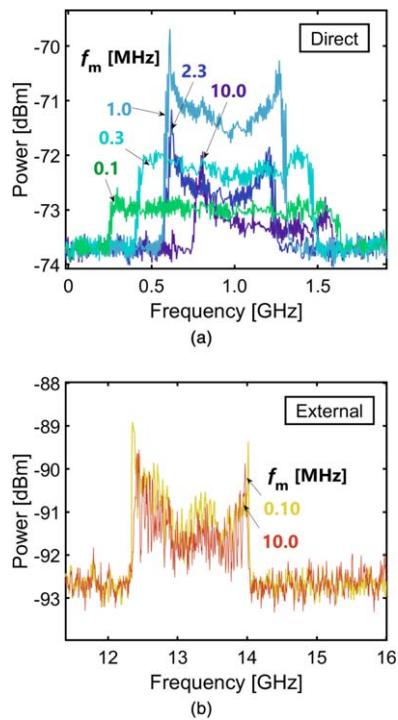


Fig. 4. (Color online) Power spectra measured at different modulation frequencies f_m . (a) Direct modulation scheme, and (b) external modulation scheme.

to ~ 1 GHz in this experiment) was observed with an ESA. The amplitude of the AC voltage applied to the laser driving current (ΔV_{LD}) was set to 2.0 V. The wavelength of the tunable laser (longer than that of the modulated laser) was adjusted so that the center frequency of the beat spectrum was located at approximately 1 GHz. The relative polarization state was optimized using a PCTRL. Averaging was performed 40 times on the ESA; the other settings were the same as those for the demonstration of the basic operation described above. In contrast, in the external modulation scheme, the output from the single laser at 1550 nm (same as the aforementioned modulated laser) was divided into two; one was externally frequency-modulated (in the figure, the downshift of the central frequency is denoted as $f_A = \sim 13$ GHz) and self-heterodyned with the other, and then the beat spectrum was observed using an ESA. The amplitude of the AC voltage applied to the VCO (V_{VCO}) was set to 2.5 V. Other settings were the same as those for the direct modulation scheme. In both experiments, the modulation frequency f_m was swept from 0.1 to 10.0 MHz (corresponding to the measurement range of OCDR from ~ 1 km down to ~ 10 m).

Figure 4(a) shows the optical spectra of the direct modulation scheme when the modulation frequency f_m was varied. When f_m increased from 0.1 to 1.0 MHz, the spectral width (corresponding to double the modulation amplitude) decreased, and the spectral power increased. This is natural if we consider that these spectra are temporally averaged and that the laser has its own response time. However, when f_m increased further to 2.3 MHz, the spectral width continuously decreased, but the spectral power decreased. When f_m increased to 10.0 MHz, the spectral width increased, the spectral power decreased, and the central frequency increased. These strange behaviors indicate that this laser is

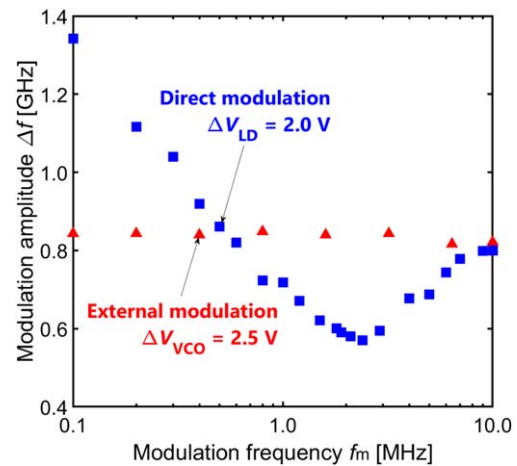


Fig. 5. (Color online) Measured dependencies of modulation amplitude Δf on modulation frequency f_m . Red triangles: direct modulation scheme, blue squares: external modulation scheme.

not suitable for high-frequency large-amplitude modulation use. In contrast, Fig. 4(b) shows the optical spectra of the external modulation scheme when f_m was 0.1 and 10.0 MHz. The shapes of the two spectra agreed well with the theory; the two spectra were almost identical from the viewpoints of the spectral width and power (the spectra measured at other f_m values were also the same). This indicates that, in the external modulation scheme, a laser not designed for special use can be employed if it satisfies such basic specifications as power, linewidth, and wavelength. Note that the power of the external modulation scheme was lower than that of the direct modulation scheme in this experiment, because the optical band-pass filter was used in the former scheme. For practical use, it should be amplified using an optical amplifier.

Finally, for quantitative evaluation, the modulation amplitude Δf (half of the spectral width) was plotted as a function of f_m for both of the modulation schemes (Fig. 5). In the direct modulation scheme, with increasing f_m , Δf was initially reduced and then increased. Thus, Δf was found to be largely dependent on f_m in the direct modulation scheme; by changing f_m , Δf could be even doubled [corresponding to two-fold reduction in the spatial resolution (from 37 to 87 mm in this range)]; such a wide-range sweeping of f_m is sometimes needed to implement specially configured OCDR systems, which exploit multiple correlation peaks simultaneously to achieve longer measurement ranges].^{34,35} In contrast, in the external modulation scheme, the fluctuations of Δf corresponding to the change in f_m were within 3% in this f_m range, proving that Δf is not largely dependent on f_m (spatial resolution: ~ 60 mm in this range). These results indicate that the interdependence of the modulation frequency/amplitude can be greatly mitigated by the external modulation scheme.

In conclusion, to tackle the disadvantages of the direct modulation scheme of SOCF-OCDR, we proposed the external modulation scheme. After confirming the basic operation, we showed that an arbitrary laser which is not designed for high-frequency large-amplitude modulation can be used in this scheme. Subsequently, we proved that the modulation frequency and amplitude are almost independent of each other in the external modulation scheme, which indicates that the spatial resolution is kept constant in the

FUT during a distributed measurement. This is not true for the direct modulation scheme, where the modulation amplitude is even doubled when the modulation frequency changed. This external modulation scheme is applicable not only to standard OADR but also to Brillouin OADR³⁾ and its two-end-access configuration, i.e., Brillouin optical correlation-domain analysis.³⁶⁾ To clarify the influence of the power modulation on the system performance will be the next important task. We believe that our proposal will be an important technique toward implementing high-performance fiber-optic correlation-domain sensing systems.

Acknowledgments The authors are indebted to Prof. Hiroyuki Uenohara, Tokyo Institute of Technology, for his experimental assistance. This work was supported by JSPS KAKENHI Grant Numbers 17H04930 and 17J07226, and by a research grant from the Fujikura Foundation.

ORCID iDs Kohei Noda  <https://orcid.org/0000-0003-4976-9657>
 Heeyoung Lee  <https://orcid.org/0000-0003-3179-0386> Yosuke Mizuno  <https://orcid.org/0000-0002-3362-4720> Kentaro Nakamura  <https://orcid.org/0000-0003-2899-4484>

- 1) A. H. Hartog, A. P. Leach, and M. P. Gold, *Electron. Lett.* **21**, 1061 (1985).
- 2) P. K. C. Chan, W. Jin, and J. M. Gong, *IEEE Photonics Technol. Lett.* **11**, 1470 (1999).
- 3) Y. Mizuno, W. Zou, Z. He, and K. Hotate, *Opt. Express* **16**, 12148 (2008).
- 4) L. Palmieri and A. Galtarossa, *J. Lightwave Technol.* **29**, 3178 (2011).
- 5) W. Zou, S. Yang, X. Long, and J. Chen, *Opt. Express* **23**, 512 (2015).
- 6) D. Huang, E. A. Swanson, C. P. Lin, J. S. Schuman, W. G. Stinson, W. Chang, M. R. Hee, T. Flotte, K. Gregory, and C. A. Puliafito, *Science* **254**, 1178 (1991).
- 7) M. A. Choma, M. V. Sarunic, C. Yang, and J. A. Izatt, *Opt. Express* **11**, 2183 (2003).
- 8) Y. Kato, Y. Wada, Y. Mizuno, and K. Nakamura, *Jpn. J. Appl. Phys.* **53**, 07KF05 (2014).
- 9) M. K. Barnoski and S. M. Jensen, *Appl. Opt.* **15**, 2112 (1976).
- 10) G. P. Lees, H. H. Kee, and T. P. Newson, *Electron. Lett.* **33**, 1080 (1997).
- 11) M. Zoboli and P. Bassi, *Appl. Opt.* **22**, 3680 (1983).
- 12) P. Healey and P. Hensel, *Electron. Lett.* **16**, 631 (1980).
- 13) Q. Zhao et al., *Sci. Rep.* **5**, 10441 (2015).
- 14) W. Eickhoff and R. Ulrich, *Appl. Phys. Lett.* **39**, 693 (1981).
- 15) D. Uttam and B. Culshaw, *J. Lightwave Technol.* **3**, 971 (1985).
- 16) B. Soller, D. Gifford, M. Wolfe, and M. Froggatt, *Opt. Express* **13**, 666 (2005).
- 17) S. Venkatesh and W. V. Sorin, *J. Lightwave Technol.* **11**, 1694 (1993).
- 18) F. Ito, X. Fan, and Y. Koshikiya, *J. Lightwave Technol.* **30**, 1015 (2012).
- 19) R. C. Youngquist, S. Carr, and D. E. N. Davies, *Opt. Lett.* **12**, 158 (1987).
- 20) E. A. Swanson, D. Huang, M. R. Hee, J. G. Fujimoto, C. P. Lin, and C. A. Puliafito, *Opt. Lett.* **17**, 151 (1992).
- 21) K. Hotate, M. Enyama, S. Yamashita, and Y. Nasu, *Meas. Sci. Technol.* **15**, 148 (2004).
- 22) Z. He, T. Tomizawa, and K. Hotate, *IEICE Electron. Express* **3**, 122 (2006).
- 23) Z. He, M. Konishi, and K. Hotate, *Proc. SPIE* **7004**, 70044L (2008).
- 24) M. Shizuka, S. Shimada, N. Hayashi, Y. Mizuno, and K. Nakamura, *Appl. Phys. Express* **9**, 032702 (2016).
- 25) M. Shizuka, N. Hayashi, Y. Mizuno, and K. Nakamura, *Appl. Opt.* **55**, 3925 (2016).
- 26) K. Hotate and O. Kamatani, *Electron. Lett.* **25**, 1503 (1989).
- 27) Z. He and K. Hotate, *J. Lightwave Technol.* **20**, 1715 (2002).
- 28) K. Hotate, *Meas. Sci. Technol.* **13**, 1746 (2002).
- 29) Z. He, H. Takahashi, and K. Hotate, Conf. Lasers and Electro-Optics (CLEO2010), CFH4, 2010.
- 30) H. Takahashi, Z. He, and K. Hotate, 36th European Conf. Exhibition on Optical Communication (ECOC2010), Tu.3.F.4, 2010.
- 31) K. Y. Song, Z. He, and K. Hotate, *Opt. Express* **14**, 4256 (2006).
- 32) K. Y. Song, Z. He, and K. Hotate, *J. Lightwave Technol.* **25**, 1238 (2007).
- 33) K. Hotate and K. Kajiwara, *Opt. Express* **16**, 7881 (2008).
- 34) Y. Mizuno, Z. He, and K. Hotate, *Opt. Express* **17**, 9040 (2009).
- 35) Y. Mizuno, Z. He, and K. Hotate, *Opt. Express* **18**, 5926 (2010).
- 36) K. Hotate and T. Hasegawa, *IEICE Trans. Electron.* **E83-C**, 405 (2000).